Heliyon 10 (2024) e33849

Contents lists available at ScienceDirect

Heliyon

journal homepage: www.cell.com/heliyon

Research article

Effect of acetylcholinesterase inhibition on immune cells in the murine intestinal mucosa

Alreem Al-Mansori [a], Ashraf Al-Sbiei [a], Ghada H. Bashir [b], Mohammed M. Qureshi [a], Saeed Tariq [c], Abeer Altahrawi [d], Basel K. al-Ramadi [b,e], Maria J. Fernandez-Cabezudo [a,e,*]

[a] Department of Biochemistry and Molecular Biology, College of Medicine and Health Sciences, United Arab University, Al-Ain, United Arab Emirates
[b] Department of Medical Microbiology and Immunology, College of Medicine and Health Sciences, United Arab University, Al-Ain, United Arab Emirates
[c] Department of Anatomy, College of Medicine and Health Sciences, United Arab University, Al-Ain, United Arab Emirates
[d] Department of Pathology, College of Medicine and Health Sciences, United Arab University, Al-Ain, United Arab Emirates
[e] Zayed Center for Health Sciences, United Arab Emirates University, Al Ain, United Arab Emirates

ARTICLE INFO

Keywords:
Acetylcholinesterase
Intestinal mucosa
Salmonella infection
Mucosal immunity
Acetylcholine

ABSTRACT

The gastrointestinal tract (GI) is the largest immune organ whose function is controlled by a complex network of neurons from the enteric nervous system (ENS) as well as the sympathetic and parasympathetic system. Evolving evidence indicates that cross-communication between gut-innervating neurons and immune cells regulates many essential physiological functions including protection against mucosal infections. We previously demonstrated that following paraoxon treatment, 70 % of the mice were able to survive an oral infection with *S. typhimurium*, a virulent strain of *Salmonella enterica* serovar Typhimurium. The present study aims to investigate the effect that rivastigmine, a reversible AChE inhibitor used for the treatment of neurodegenerative diseases, has on the murine immune defenses of the intestinal mucosa. Our findings show that, similar to what is observed with paraoxon, administration of rivastigmine promoted the release of secretory granules from goblet and Paneth cells, resulting in increased mucin layer. Surprisingly, however, and unlike paraoxon, rivastigmine treatment did not affect overall mortality of infected mice. In order to investigate the mechanistic basis for the differential effects observed between paraoxon and rivastigmine, we used multi-color flowcytometric analysis to characterize the immune cell landscape in the intraepithelial (IE) and lamina propria (LP) compartments of intestinal mucosa. Our data indicate that treatment with paraoxon, but not rivastigmine, led to an increase of resident $CD3^{+}CD8^{+}$ T lymphocytes in the ileal mucosa (epithelium and lamina propria) and $CD11b^{-}$ $CD11c^{+}$ dendritic cells in the LP. Our findings indicate the requirement for persistent cholinergic pathway engagement to effect a change in the cellular landscape of the mucosal tissue

Abbreviations: ***ACh***, acetylcholine; ***AChE***, acetylcholinesterase; ***CFUs***, colony forming units; ***ChAT***, choline acyl transferase; ***DAB***, diaminobenzidine; ***DCs***, dendritic cells; ***ENS***, enteric nervous system; ***GI***, gastrointestinal; ***IBD***, inflammatory bowel disease; ***IE***, intraepithelial; ***IELs***, intraepithelial lymphocytes; ***IFN-γ***, interferon-gamma; ***ILCs***, innate lymphoid cells; ***IL-17***, interleukin 17; ***LP***, lamina propria; ***LPLs***, lamina propria lymphocytes; ***mAChR***, muscarinic acetylcholine receptors; ***nAChR***, nicotinic acetylcholine receptors; ***NK***, natural killer cells; ***STZ***, streptozotocin; ***Th17***, T helper-17; ***TNFα***, tumor necrosis factor alpha.

* Corresponding author. Department of Biochemistry and Molecular Biology College of Medicine & Health Sciences United Arab Emirates University Al-Ain, United Arab Emirates.
E-mail address: mariac@uaeu.ac.ae (M.J. Fernandez-Cabezudo).

https://doi.org/10.1016/j.heliyon.2024.e33849
Received 1 March 2024; Received in revised form 27 June 2024; Accepted 27 June 2024
Available online 28 June 2024

that is necessary for protection against lethal bacterial infections. Moreover, optimal protection requires a collaboration between innate and adaptive mucosal immune responses in the intestine.

1. Introduction

The mean total surface area of the gastrointestinal (GI) mucosal system in human adults has been estimated at ~32 m^2, which is amplifiable by a factor of ~100 b y the presence of villi and microvilli along the small and large intestines [1]. This large surface area facilitates the three main functions of the GI tract, namely digestion and absorption of nutrients, defense against invading pathogens, and continuous interaction with the commensal microbiota that molds and maintains immune homeostasis along the tract. Host defense along the GI tract utilizes non-immune as well as immune innate and adaptive mechanisms that encompass discrete lymphoid compartments, including the Peyer's patches, lamina propria (LP) and intraepithelial lymphocytes (IELs) [2].

Salmonella enterica is one of the most common bacterial enteropathogens and the etiologic agent of salmonellosis and typhoid fever in humans. There are over 2600 Salmonella bacteria serotypes [3], being *Salmonella enterica* subsp. *Salmonella enterica* subsp. Enterica serovars Typhi and Paratyphi are the causative agents of Typhoid fever which accounted for ~9 million cases and 110,00 deaths in 2019 alone (https://www.who.int/news-room/fact-sheets/detail/typhoid). *Salmonella enterica* serovar Typhimurium is responsible for salmonellosis, or food poisoning, in humans and over 91,000 salmonellosis cases are reported each year in the EU. It has been estimated that the overall economic burden of human salmonellosis is as high as €3 billion a year (European Food Safety Authority, 2024). Infection usually occurs from eating contaminated foods (dairy, eggs, meat, raw product), drinking contaminated water or from contact with infected persons. Despite the efforts to prevent and control *Salmonella* enterica infections in humans, by avoiding contamination in animals, vegetables and fruits, the prevalence of Salmonella infections is still high. Moreover, antimicrobial resistance in *Salmonella* strains is of concern for public health safety as it led to inability to treat the disease [4]. Furthermore, the developed vaccines are ineffective in preventing the infection [5]. Therefore, a new approach is needed to deal with bacterial infections.

The GI tract is innervated by the enteric nervous system (ENS) composed of the myenteric and submucosal plexuses. Additionally, the GI tract receives extrinsic innervation by neurons of the sympathetic, parasympathetic (mainly vagal) and visceral nervous systems [6]. Direct vagal innervation has been described in the intestinal mucosa specifically between the intestinal crypts, the villous lamina propria reaching the basal membrane, but without making direct contact with epithelial cells [7,8]. Vagal stimulation leads to the release of acetylcholine (ACh) that acts on neurons of the ENS inducing the release of neuropeptides and neurotransmitters.

Numerous immune cell populations, including lymphocytes, macrophages and dendritic cells, express ACh receptors (muscarinic and/or nicotinic) [9–11] which suggests that ACh could directly modulate the immune response. Lymphoid cells such as T cells, B cells, dendritic cells and macrophages, express ChAT (choline acetyltransferase) and release ACh in response to different signals [12,13]. Given that ACh is the major neurotransmitter in the cholinergic nervous system, and could potentially mediate communication between immune cells, suggests that ACh may play a central role in the interaction between the nervous and immune systems. In this context, Tracey and co-workers demonstrated that the inflammatory response is modulated by the existing collaboration between the nervous and immune systems, a concept known as the *inflammatory reflex* [14,15].

Although the anti-inflammatory effect of cholinergic stimulation has been demonstrated by various groups of investigators [16–23], the underlying mechanisms are not completely understood. At the level of the spleen, cholinergic stimulation induced the production of ACh by $CD4^+$ T cells [12,24], which in turn binds to nicotinic acetylcholine receptors (nAChR) on macrophages [25] and reduce the production of pro-inflammatory cytokines, including TNFα. At the level of the pancreas and using the streptozotocin (STZ)-induced diabetic murine model, our laboratory demonstrated that acetylcholinesterase (AChE) inhibition avoided pancreatic beta-cell destruction and, therefore, the increase of glucose levels in blood in STZ-treated animals. This observation was correlated with a change in the type of immune response induced by STZ, that shifted from a predominant interleukin 17 (IL-17) to an interferon gamma (IFNγ) response [21]. The effect of AChE inhibition was also evident at the level of the GI mucosa, where it was found to induce anti-microbial innate immune defenses, leading to an enhanced survival of animals that received a lethal dose of *S. typhimurium* [26,27].

In all our aforementioned studies [21,26–28], modulation of ACh release was achieved through long-term administration of a highly selective and non-reversible inhibitor of the AChE enzyme, namely paraoxon. AChE hydrolyzes ACh in the synaptic cleft, hence increasing the levels of ACh available for postsynaptic stimulation [29]. However, given that paraoxon is not a physiologically designed AChE inhibitor, in the present study we aimed to analyze the efficiency of rivastigmine, an AChE inhibitor used for the treatment of neurodegenerative diseases, in the murine *Salmonella* infection model, and compare the effects that treatment with either paraoxon or rivastigmine exert on the immune cells that populate the mucosa in the intestine (SFig. 1) . We hypothesized that rivastigmine could have the same effect as paraoxon on the intestinal mucosa and, therefore, improve survival following a lethal infection.

Our findings show that treatment with rivastigmine increased median survival of *S. typhimurium* infected mice and appears to delay the spread of pathogenic bacteria to other parts of the body. Importantly, however, rivastigmine failed to rescue the animals from succumbing to the infection, which was in sharp contrast to the overall effect previously observed with paraoxon. To gain an understanding of the requirements for host protection, we undertook a detailed analysis of the mucosal innate and adaptive immune system compartments following treatment with paraoxon or rivastigmine. Our findings indicate that rivastigmine and paraoxon induced similar innate immune responses which includes the secretion of granules from Paneth cells and goblet cell that resulted in an increase in the thickness of the mucin layer in the colon. However, the distribution of immune cells at the effector sites of the LP and IELs was distinct following the two treatments. These findings suggest that a more persistently stable AChE inhibition is required to

increase surveillance and prepare the intestinal mucosa for rapid control of microbial proliferation following infection with a virulent oral pathogen.

2. Materials and methods

2.1. Experimental animals

BALB/c mice were purchased from the Jackson Laboratory (Bar Harbor, ME, USA) and bred in the animal facility at the College of Medicine and Health Science, United Arab Emirates University [27]. Male mice aged 8–12 weeks were used for all experiments in accordance, and after approval of the animal research ethics committee of the College of Medicine and Health Science, United Arab Emirates University (Protocol no. AE/06/81).

2.2. Acetylcholinesterase inhibitors

Paraoxon ethyl and rivastigmine were purchased from Sigma (St Louis, MO). A stock solution of 10 mmol/L paraoxon was prepared in anhydrous acetone and then diluted to 1 mmol/L in PBS. Ex tempore, a solution of 80 nmol/ml of paraoxon in PBS was prepared in order to deliver 40 nmol/mouse by daily intraperitoneal (i.p) injection (equivalent to 0.44 mg/kg of body weight).

A stock solution of 50 mg/ml rivastigmine was prepared in DMSO and then diluted to a concentration of 17.7 μg/μl in PBS from which mice received 200μl/mouse/day by subcutaneous (s.c) injection (equivalent to 2 mg/kg). Mice in the control group received daily injections of PBS.

2.3. Bacterial preparation and inoculation

SL1344 strain of *S. typhimurium* was utilized in this study. Preparation of log-phase bacteria has been already described elsewhere [26,27,30,31]. SL1344 was administered by oral inoculation in 200 μl/mouse following already described protocol [26]. Bacterial dose was confirmed by colony-forming units (CFUs) plate counts. All experiments using *Salmonella* were performed following institutional biohazard regulations in a BSL2 laboratory.

2.4. Experimental protocol

Male mice age- and weight-matched BALB/c were randomly divided into three groups with 5 mice/group/experiment. *Group I* received daily injections of sterile saline and served as control. *Group II* received daily injections of paraoxon and *Group III* daily injections of rivastigmine. Treatments were administered for three consecutive weeks with five injections per week with two days rest [27]. Once a week, mice were weighted and, in control and paraoxon-treated mice, blood collected and analyzed for AChE activity in red blood cells. After the three-week treatments and following the 2-day break, animals were either sacrificed (groups I, II and III) or infected with virulent bacteria (SL1344) and euthanized at the specified time points (groups I and III). In other experiments the survival of infected animals was monitored. Fig. 1A shows the timeline and experimental procedures.

2.5. Calculation of bacterial counts

On day three post infection, fecal pellets were freshly collected and, after being weighed, were placed in 1 ml cold PBS and homogenized. Afterwords, mice were sacrificed and internal organs (liver, spleen and intestine) as well as the intestinal content were obtained, placed in 1 ml cold PBS and homogenized. Crude or diluted homogenates (100 μl) were cultured at 37 °C on plates of SS agar with streptomycin (200 μl/ml). After overnight incubation, CFUs were calculated.

2.6. Isolation of intraepithelial and lamina propria lymphoid cells from the intestine

Following the treatment with saline, paraoxon or rivastigmine, mice were euthanized, and small intestines collected and cleaned of fecal content, fat tissue and Peyer's patches before being weighed. Intestines were opened longitudinally, cut into small pieces and incubated with pre-digestion solution (HBSS w/o Ca^{++} and Mg^{++}). Then, intestinal tissue was filtered, and supernatant collected. This procedure was repeated three times and, supernatant pulled, centrifuge and pellet containing IELs resuspended in PBS. For the isolation of LP leukocytes (LPLs), remaining intestinal tissue was further digested using the lamina propria dissociation kit (Miltenyi Biotec, Bergisch Gladbach, Germany) and the gentleMACS dissociator (Miltenyi Biotec), following manufacturer protocol.

2.7. Flow cytometric analysis

Isolated IELs and LPLs were analyzed using FACS and following standard protocol [27]. Cells were stained with different combinations of conjugated monoclonal antibodies CD3-BV785, CD4-PE, CD8α-APC/Fire750, CD8β-FITC, CD11b-Alexa Fluor 488, CD11c-APC or PE, CD19-PE-Dazzle594, CD45-PE or APC, CD103-BV421 and γδTCR- BV605 (All from BioLegend, San Diego, CA, USA). Non-viable cells that stained positive for Zombie Aqua Viability Dye-BV-510 (BioLegend), were excluded from the analysis. For each antibody, an appropriate isotype control was used. Data were collected on 30,000 cells using BD FACS Celesta (BD Biosciences,

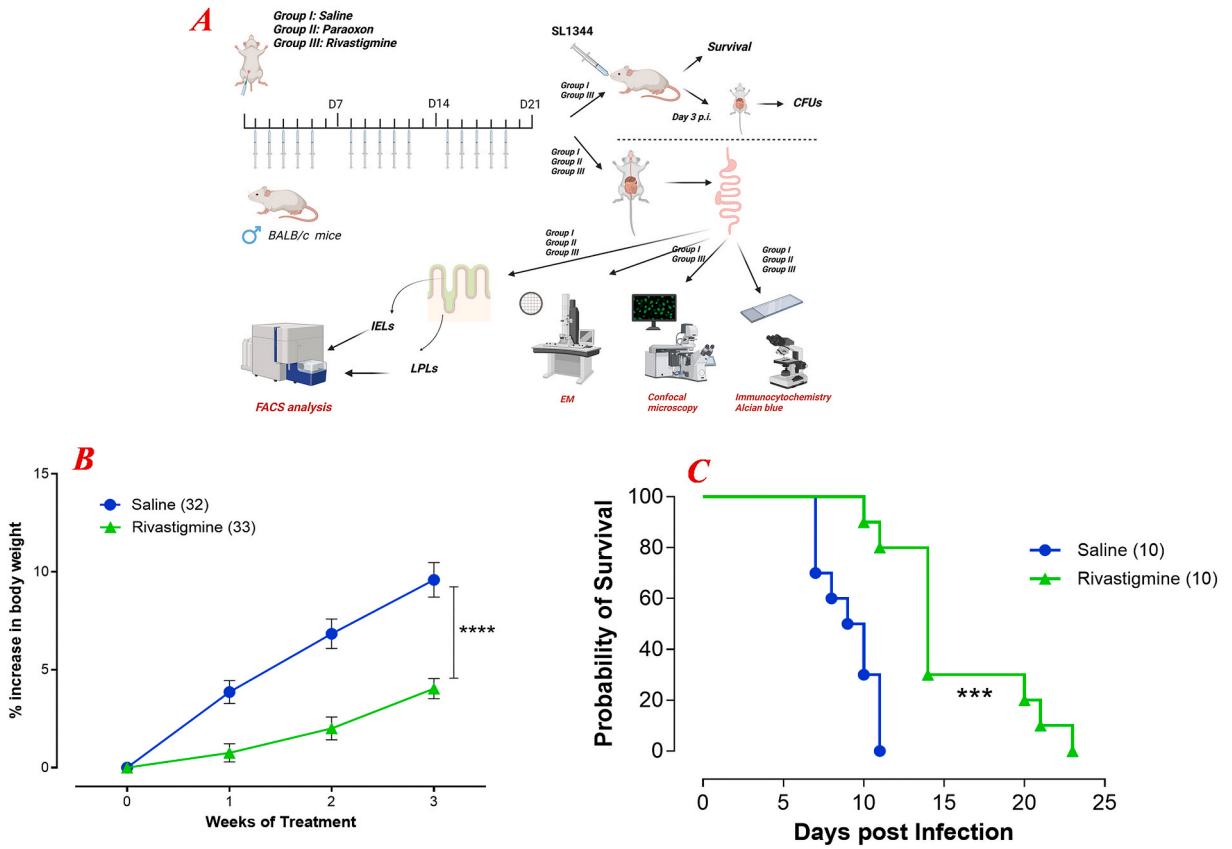

Fig. 1. Rivastigmine treatment reduced body growth and improved survival to oral infection with virulent *S. typhimurium*. (***A***) Graphic representation of the experimental timeline and procedures (Created with BioRender). During the three-week treatment with saline or rivastigmine, mice were weighed weekly, and (***B***) body weight gain calculated as percentage of the initial weight. Graph shows the mean values ± SEM of data pooled from 5 independent experiments (n = 33–32 mice/group). Asterisks denote statistically significant differences between the control and experimental group ****$p < 0.0001$. (***C***) After the treatments with saline or rivastigmine, animals received an oral infection with SL1344 (2×10^4 CFUs/mouse). Survival was followed for up to 30 days after infection. Graph depicts the mean ± SEM of pooled data from two independent experiments (n = 10/group). Chi squared (Mantel-Cox) statistical test was used for this analysis. Asterisks denote statistically significant differences between the control and experimental group (***$p < 0.001$).

Franklin Lakes, NJ, USA) and analyzed using FlowJo software (Ashland, OR, USA).

2.8. Histological investigation of the intestine

Ileum was removed and prepared for histological studies following established protocol. To visualize the acid mucins in the intestinal lumen, colon was excised and fixed using Carnoy's solution. Colon sections were stained using 1 % (w/v) Alcian blue 3GX (Sigma, Saint Louis, MO, USA), differentiated in tap water, counter-stained with hematoxylin (Thermo Fisher Scientific, Waltham, MA, USA) and visualized with an Olympus BX51 microscope equipped with digital camera DP26 (Olympus Corporation, Tokyo, Japan). Mucin thickness in the intestinal lumen was measured in 3–4 high power fields (HPF)/section using 2–5 sections/mouse. A 3-steps staining protocol was followed to detect B cells, T cells (CD4 and CD8) as well as cells producing IFNγ on ileum sections. For B lymphocytes, anti-CD45R (BD, Franklin Lakes, NJ, USA) rat monoclonal antibody was used and followed by a secondary anti-rat HRP (Abcam) and DAB (Dako, Carpinteria, CA, USA). For CD4 and CD8 T lymphocytes as well as IFNγ-producing cells, rabbit anti-CD4, anti-CD8 and anti-IFNγ (all from Abcam, Cambridge, UK), respectively, were used followed by anti-rabbit HRP (Cell signaling, Danvers, MA, USA) and DAB. Sections were counter-stained with hematoxylin and visualized, and photographed, with an Olympus BX51 microscope equipped with digital camera DP26 (Olympus Corporation, Tokyo, Japan). Quantification of labeled cells was performed in 10 HPF/section using 2–3 section/mouse. $CD4^+$ and $CD8^+$ cells in LP and epithelium were counted separately. $CD45R^+$ and $IFN\gamma^+$ cells were difficult to determine their exact location within the intestinal mucosa for which these cells were quantified as mucosal cells without specifying the exact location.

Indirect immunostaining for mucin and lysozyme was performed using rabbit polyclonal anti-mucin (Santa Cruz Biotechnology, Santa Cruz, CA, USA) and anti-lysozyme (Dako, Glostrup, Denmark), respectively, followed in both cases by FITC-conjugated donkey anti-rabbit IgG (Jackson ImmunoResearch, West Grove, PA, USA). All sections were counter-stained with propidium iodide (BD

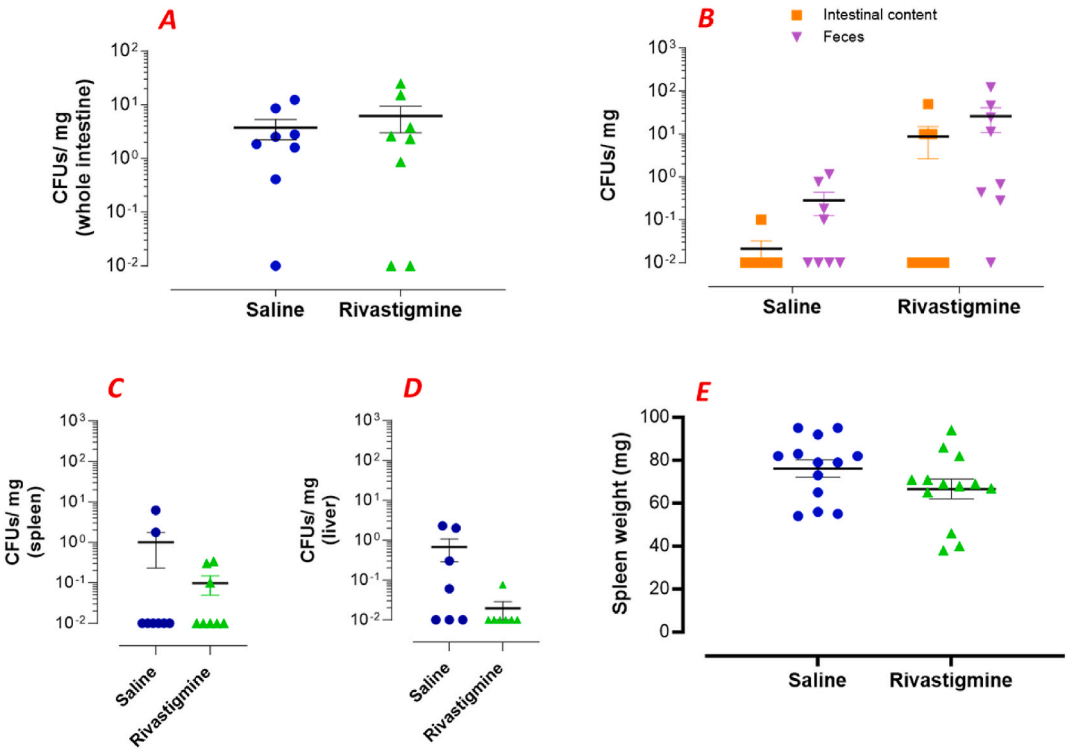

Fig. 2. Rivastigmine treatment reduced bacterial counts in systemic organs at day 3 post infection. After saline or rivastigmine treatment, mice received an oral infection with SL1344 (1×10^5 CFUs/mouse). Three days after infection, mice were euthanized, organs collected and homogenized. Homogenate aliquots were plated, and bacterial counts calculated as CFUs/mg in **(*A*)** whole intestine, **(*B*)** feces and intestinal content as well as **(*C*)** spleen and (***D***) liver. Graphs show individual values and mean ± SEM from 2 independent experiments (n = 8 mice/group). Spleens were weighted before homogenization, and individual values and mean ± SEM from 3 independent experiments (13 mice/group) plotted in graph ***E***. Student's t-test was used for data analysis. No statistically significant differences between the control and experimental group were found in any of the graphs.

Bioscience) and examined and photographed under a Nikon C1 laser scanning confocal microscope. For electron microscopy study, tissue was fixed, and prepared following a published protocol [27]. Sections were examined and photographed with TENAI G2 Spirit Transmission Electron Microscope (FEI, Hillsboro, OR, USA).

2.9. Quantitative RT-PCR analysis

RNA from IELs and LPLs was extracted by TRIzol method and repurified on Qiagen columns (RNA easy mini kit, Qiagen, Valencia, CA). cDNA was synthesized using TaqMan reverse transcription reagents (Applied Biosystems, Foster City, CA) according to manufacturer's protocol. Premade Taqman primers and probes (Applied Biosystem) were used to study the expression of INFγ and HPRT. Transcript levels of target gen were normalized according to the ΔCq method to respective mRNA levels of the housekeeping gen HPRT. The expression of the target gene is reported as the level of expression relative to HPRT.

2.10. Statistical analysis

Statistical significance between control and treated groups was analyzed by unpaired two-tailed Student's t-test or one-way ANOVA. For survival analysis, the log rank (Mantel-Cox) test for Kaplan-Meier functions was applied. GraphPad Prism software (San Diego, CA, USA) was utilized for the analysis. p values < 0.05 denoted significant differences between the experimental groups.

3. Results

3.1. Rivastigmine treatment reduced body weight growth

The choice of rivastigmine over other AChE inhibitors was based on its selective inhibitory action on AChE and BChE. Galantamine is a weaker AChE inhibitor than rivastigmine and can also modulate nicotinic ACh receptors allosterically. Moreover, donepezil not only acts as an AChE inhibitor, but it also upregulates nicotinic AChR in neurons. Therefore, in order to avoid any effect on nicotinic

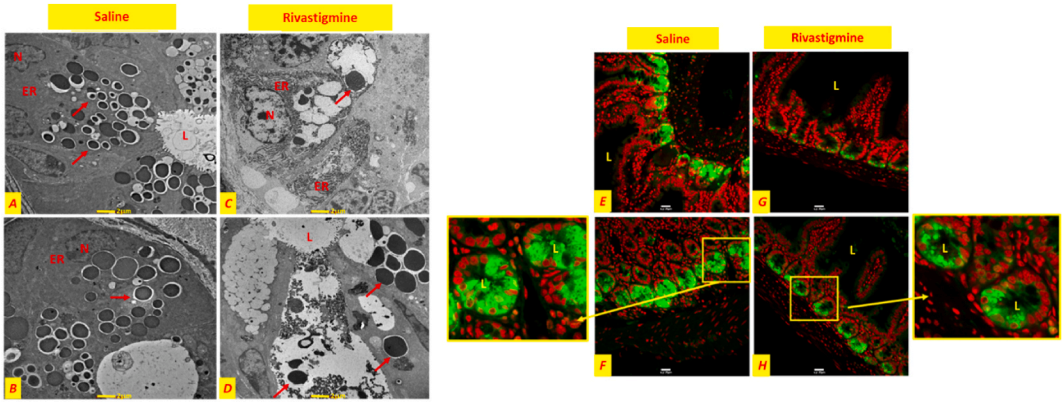

Fig. 3. Rivastigmine induced Paneth cells' degranulation and release of lysozyme. (***A-D***) Electron microscopy pictures of ileum crypts. (***A-B***) Paneth cells from saline treated mice contain numerous protein-containing vesicles (arrows) and a prominent endoplasmic reticulum. (***C-D***) After rivastigmine treatment, the secretory granules in Paneth cells are fused and show irregular structure. **ER**: endoplasmic reticulum; **L**: intestinal lumen; **N**: nucleus. Scale bar = 2 μm. (***E-H***) Paraffin-embedded sections from the ileum were stained with anti-lysozyme antibody. (***G,H***) Rivastigmine treatment resulted in a reduction in the intensity of positively labeled (green) Paneth cells when compared to control group (***E,F***). Side panels in images ***F*** and ***H*** are magnified pictures of their respective delineated areas. Sections were counterstained with propidium iodide (red) ***L***: lumen. Scale bar = 20 μm. All photos are representative of 3–5 mice/group from 2 independent experiments.

ACh receptors, we decided to use rivastigmine for the current study.

Treatment with AChE inhibitors is associated with a transient weight loss [21,32]. To monitor the efficiency of rivastigmine treatment, mice were weighted weekly during the 3-week treatment period. Fig. 1B depicts the body weight gain of mice treated with saline or rivastigmine. Saline-treated mice showed a gradual increment in their body weight. However, rivastigmine-treated mice showed a significant decrease in body weight gain during the treatment, which is in line with the expected effect of AChE inhibitors.

3.2. Rivastigmine exposure improved overall survival following a lethal infection

The highly specific and irreversible AChE inhibitor, paraoxon, was previously shown to increase resistance to mucosal infection by virulent Salmonella (strain SL1344) [26,27]. To assess whether rivastigmine could act similarly, mice pretreated with saline or rivastigmine were orally infected with SL1344 (2×10^4 CFUs/mouse). Mice were followed for 30 days post-infection to determine overall survival. Rivastigmine administration led to a significant enhancement in survival (median survival increased from 9.5 days in saline group to 14 days) (Fig. 1C). Despite the improved survival, however, all mice in both the saline and rivastigmine groups eventually died from the infection, signifying the level of virulence of the Salmonella strain used in this study.

3.3. Rivastigmine reduced bacterial dissemination

Next, we investigated the presence of bacteria in the intestinal mucosa as well as in organs such as liver and spleen. Following saline or rivastigmine treatment, mice were orally infected with SL1344 (1×10^5 CFUs/mouse) and euthanized 3 days later. Bacterial counts in spleen, liver, fecal pellet as well as in the intestinal content and total intestine, were calculated. No differences in bacterial counts in the whole intestine (including content and tissue) were detected between the saline and rivastigmine groups. (Fig. 2A). However, the number of bacteria in the intestinal content and feces was lower in the saline-treated group than in the rivastigmine-treated group (Fig. 2B). In contrast, the bacterial load in liver and spleen was higher in saline group than in rivastigmine-treated group (Fig. 2C and D). Our results suggest that bacterial translocation and dissemination was initially prevented by rivastigmine treatment. The extent of splenomegaly was also assessed in the two experimental groups. The average spleen weight in saline-treated group was 76 ± 4.1 mg (mean ± SEM) slightly larger than in rivastigmine-treated mice (65 ± 4.6 mg) (Fig. 2E), possibly reflecting the reduction in bacterial translocation across the intestinal mucosa in the latter group. However, the differences in all the reported parameters between the saline and rivastigmine groups did not reach statistical significance, most likely due to the fact that mice were sacrificed only 3 days after infection.

3.4. Rivastigmine induced the release of lysozyme and mucin

Next, we investigated the potential changes that rivastigmine exerted in the intestinal mucosa as we have previously observed following paraoxon treatment [27]. Specifically, we wanted to see if we could detect any changes in the morphology of the intestinal mucosa that could explain the delay observed in bacterial translocation in rivastigmine-treated mice. Ultrastructural observation of intestinal tissue from saline-treated mice revealed healthy Paneth cells with nucleus at the basal part, a well-developed endoplasmic reticulum and multiple granules of different sizes frequently surrounded with clear halos (Fig. 3A and B). In contrast, examination of ileal tissue from rivastigmine-treated mice showed Paneth cells with atypical morphology, with evidence of stressed endoplasmic

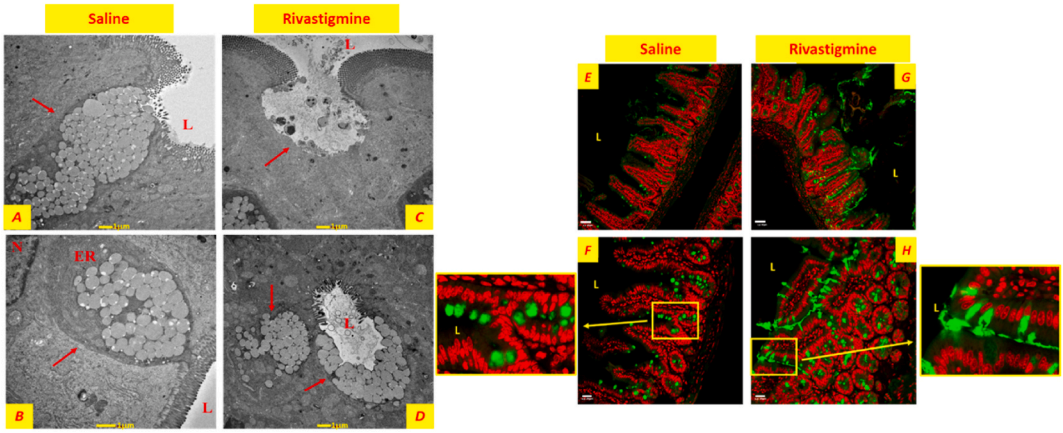

Fig. 4. Rivastigmine induced goblet cells' degranulation. Electron microscopy pictures of ileum epithelium from mice treated with (***A-B***) saline or (***C-D***). In control mice, goblet cells (arrows) contain numerous mucous globules in their cytoplasm. Rivastigmine treatment induces degranulation of goblet cells and mucus secretion. Bar = 1 μm. (***E-H***) Paraffin-embedded sections from the ileum were stained with anti-mucin antibody. Confocal micrographs show the mucin content in the cytoplasm of goblet cells (green) in (***E,F***) saline and (***G,H***) rivastigmine-treated mice. Delineated zones (***F, H***) have been enlarged in the side panels. Scale bar = 40 μm in ***E and G.*** Scale bar = 20 μm in ***F*** and ***H***. All photos are representative of 3–4 mice/group from 2 independent experiments. **L**: intestinal lumen; **ER**: endoplasmic reticulum.

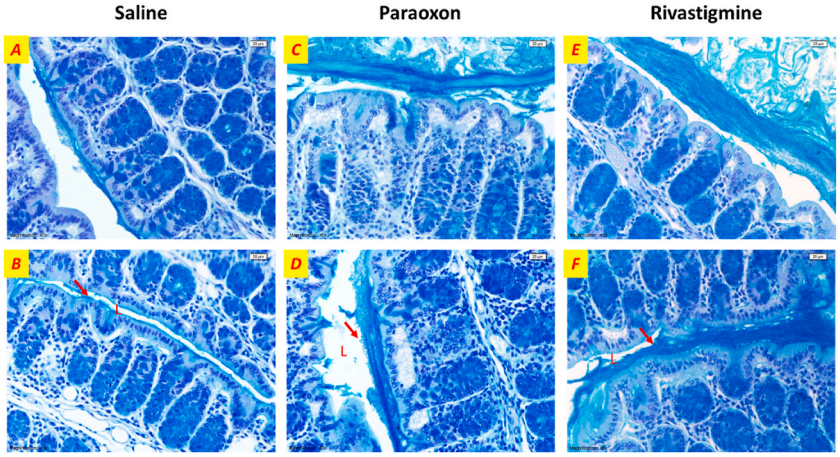

Fig. 5. AChE inhibition results in a thicker colonic mucin. Mice treated with saline, paraoxon or rivastigmine were sacrificed. Colon excised, processed and stained with Alcian blue for mucin content visualization. Colon of mice treated with saline (***A, B***) show an intestinal lumen with a thin mucin layer (arrow). In contrast, (***C,D***) paraoxon and (***E,F***) rivastigmine treatment resulted in a much thicker layer of mucin. Scale bars at the top right corner of the picture = 20 μm. Pictures are representative of 3 slides/mouse, 4 mice per group from 3 independent experiments. **L**: lumen.

reticulum and large vacuoles (Fig. 3C). Some of these cells were devoid of any granules and presented with an apparently empty cytoplasm opened to the intestinal lumen (Fig. 3D). We next investigated if these structural modifications in Paneth cells were affecting their lysozyme content. Lysozyme is one of the antimicrobial proteins that Paneth cells produce and secrete in response to microbial interaction. Confocal microscopy of intestinal sections from control mice revealed Paneth cells with cytoplasm filled with lysozyme, revealed by an intense pattern of staining (Fig. 3E, F). However, sections from rivastigmine-treated group showed Paneth cells that exhibited a weak lysozyme staining (Fig. 3G, H) which indicates that lysozyme has been released, corroborating the results observed by ultramicroscopy.

Goblet cells constitute a prominent cell population present in the epithelium of the intestine. By electron microscopy, goblet cells appeared scattered in between adjacent intestinal epithelial cells. In the saline control group, goblet cells were big with a cup shaped structure, and highly polarized. The nucleus was located at the base of the cells together with a well-developed endoplasmic reticulum, and an apical side filled with membrane-bound granules (Fig. 4A, B). In the rivastigmine-treated group, goblet cells were completely or partially depleted of granules and appeared to release their content to the intestinal lumen (Fig. 4C, D). In some goblet cells the secretion seemed to be very forceful to the extent that the cell membrane was disrupted. Given that mucin is the most abundant bioactive molecule synthesized by intestinal goblet cells, we analyzed the mucin content and goblet cell degranulation by confocal microscopy using a specific anti-mucin antibody. In saline-treated mice, labeled goblet cells appeared rounded in shape with a dense

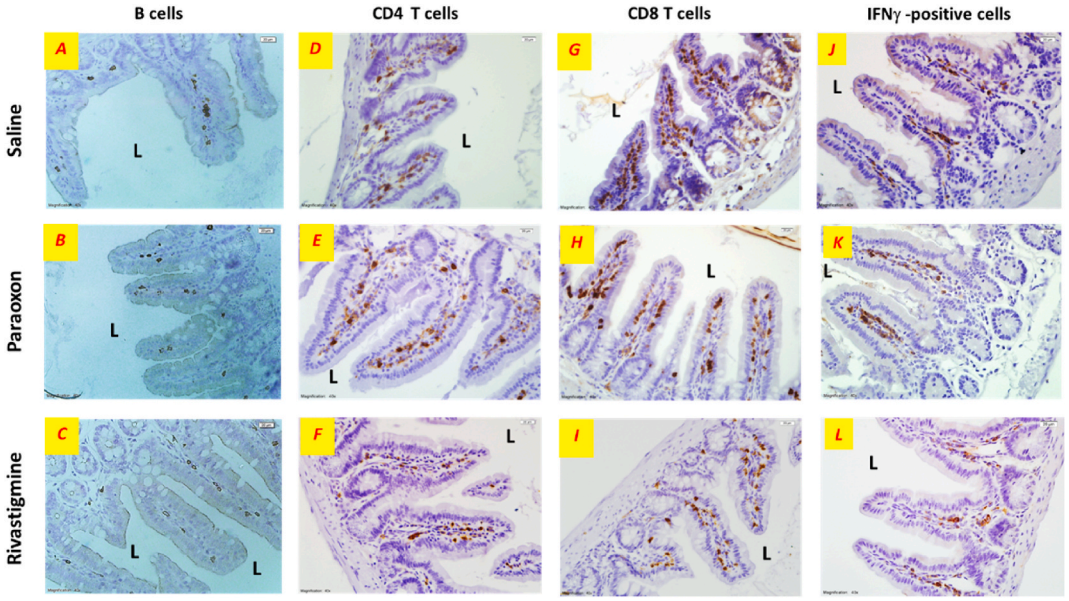

Fig. 6. Immunohistochemical study of immune cells in the intestinal mucosa. Ileum sections obtained from (***A, D, G, J***) saline- (***B, E, H, K***) paraoxon- and (***C, F, I, L***) rivastigmine-treated mice were stained with (***A-C***) anti-CD45R, (***D-F***) anti-CD4, (***G-I***) anti-CD8 and (***J-L***) anti-IFNγ antibodies, as described in *Material and Methods* section, and counterstained with hematoxylin. Images show immune-positive, dark brown-stained cells. Scale bars at the top right corner of the picture = 20 μm. Photos are representative of 3–5 mice/group from 3 independent experiments. ***L*:** intestine lumen.

stained cytoplasm (Fig. 4E, F). In contrast, immunostaining of ileum of rivastigmine-treated mice revealed goblet cells with their apical side opened and releasing their content to the intestinal lumen (Fig. 4G, H).

As a result of this degranulation, we hypothesized that the mucin layer coating the intestinal epithelium should be more prominent after treatment with AChE inhibitors. Previous work demonstrated that along the intestinal tract, there is a variation in the percentage of goblet cells which is directly correlated to the size of the mucin layer, being more abundant in the colon than in the small intestine [33]. Therefore, to better visualize any changes in the intestinal mucus layer induced by paraoxon and rivastigmine, we studied the proximal part of the colon. Following the treatment with saline or AChE inhibitors (paraoxon or rivastigmine) colon was excised and processed for histological analysis to detect the presence of epithelial mucins. The saline-control group showed a thin colonic mucus layer (Fig. 5A and B) compared to the many layers found in the intestinal lumen of paraoxon- (Fig. 5C and D) and rivastigmine- (Fig. 5E and F) treated groups. This fact was further investigated by measuring the depth of the mucin layer in the colon sections of each group (SFig. 2). The results confirmed a statistically significant increase in the intestinal mucin layer in the paraoxon and rivastigmine groups compared to the saline group. Taken together, these morphological findings demonstrate that both rivastigmine and paraoxon act similarly, and effectively induce the release granules from Paneth cells, causing the secretion of anti-microbial effector molecules, and goblet cells which leads to an increase in the intestinal mucus layer.

3.5. *Immunohistochemical analysis of mucosa-associated immune cells*

Paraoxon and rivastigmine share the property of inducing the release of mucin and lysozyme from goblet and Paneth cells, respectively, but yet rivastigmine was unable to induce the same level of protection against SL1344. This suggests that other alterations along the mucosal tract could underlie the observed protective effect. In the next series of studies, we focused on the potential changes induced by each of the AChE inhibitors on the lymphoid populations of the intestinal mucosa. Immunohistochemical staining of ileum sections from saline-, paraoxon- or rivastigmine-treated group was carried out to assess any potential alterations in lymphocyte numbers and location. Analysis of B cells in ileal sections revealed their presence mainly in the LP (Fig. 6A–C), where similar cell numbers per HPF were determined in all three experimental groups (SFig. 3A). $CD4^+$ T cells were also mostly located in the LP (Fig. 6D–F) while $CD8^+$ T cells were more abundant (~2-fold) in the intraepithelial (IE) compartment compared to the LP (Fig. 6G–I). While there were significant differences between the number of CD4 T cells in IE vs. LP compartments (SFig. 3B), there were no significant differences in their numbers within each compartment following each treatment. Likewise, the abundance of CD8 T cells in the IE was clearly statistically different than in the LP compartment (SFig. 3C). However, no statistically significant difference was found in their abundance within each compartment following treatment.

Considering the essential role that the proinflammatory cytokine IFNγ plays in the defense against *Salmonella* infection [34], we investigated the presence and location of cells that produce IFNγ-in the ileal mucosa. Immunostaining with an anti-IFNγ antibody showed $IFN\gamma^+$ cells among the epithelial cells and at the basal surface adjacent to the underlying tissue (Fig. 6J-L). Quantification of $IFN\gamma^+$ cells at HPF reveled a small increment induced independently by both AChE inhibitors (16.3 ± 1.9 and 16.1 ± 1.5 cells per HPF,

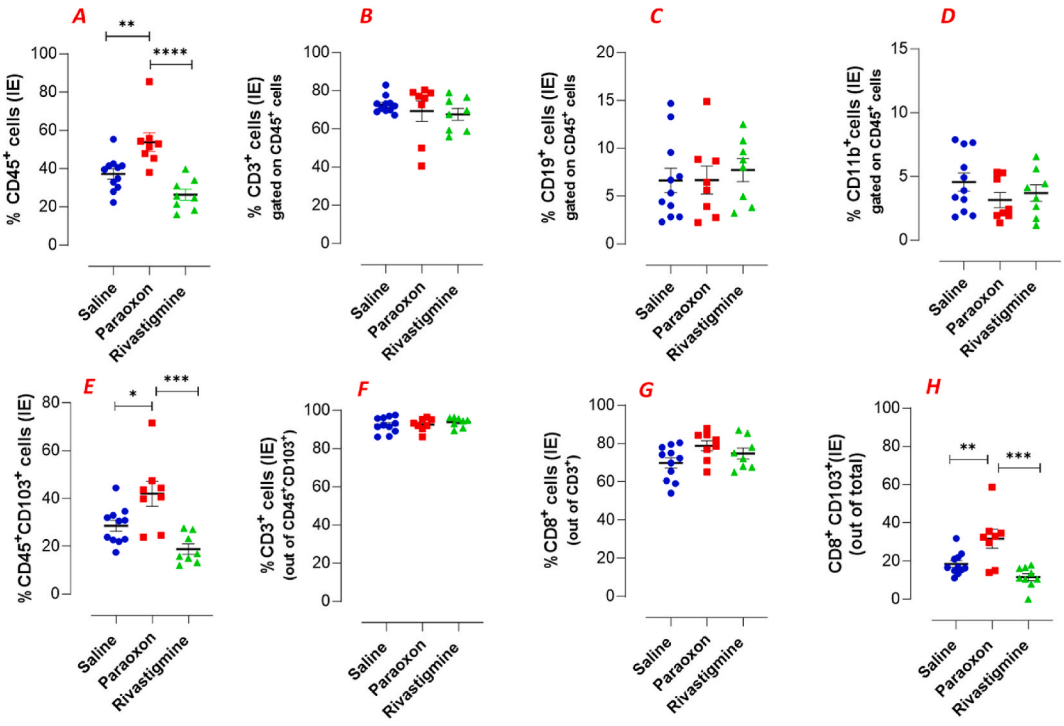

Fig. 7. Paraoxon treatment resulted in an increase in resident hematopoietic cells of CD8 phenotype in the intestinal epithelium. After 3 weeks of treatment with saline, paraoxon or rivastigmine, mice were sacrificed. Isolated intraepithelial (IE) cells from ileum were analyzed by flowcytometry using specific mAbs. (***A-D***) Graphs show the percentage of (***A***) total $CD45^+$ cells and its three main populations: (***B***) $CD3^+$ T cells, (***C***) $CD19^+$ B cells and (***D***) $CD11b^+$ myeloid cells in the epithelium of saline-, paraoxon- and rivastigmine-treated mice. Graphs ***E-G*** depict the percentages of resident IE (***E***) hematopoietic cells $CD45^+CD103^+$ (***F***) $CD3^+$ T cells and (***G***) $CD8^+$ T cells. Graph ***H*** shows the percentage of $CD8^+CD103^+$ cells out of the total IE population. All graphs represent individual values and the mean ± SEM of 7–10 mice per group from 3 independent experiments. One-way ANOVA statistical test was used for data analysis. Asterisks denote statistically significant differences between groups (*$p < 0.05$; **$p < 0.01$; ***$p \leq 0.001$; ****$p < 0.0001$).

in paraoxon and rivastigmine, respectively) compared to saline-treated group (13.2 ± 1.4 cells/HPF) (SFig. 3D). However, this difference was not significant. To confirm this result, we carried out qRT-PCR analysis of purified IELs and LPLs. The data revealed a very low level of expression of IFNγ by both cell types. Importantly, there were no significant differences between control and drug-treated mice (SFig. 4).

Therefore, treatment with paraoxon or rivastigmine did not appear to modify the normal distribution of lymphoid cells in the ileum. Moreover, quantitative differences were not observed among the three treatment groups.

3.6. Phenotypic analysis of the mucosal immune populations by flowcytometry

In order to determine the possible changes in intestinal immune cell populations following AChE inhibition more quantitatively, the immune cell phenotypes in the intestinal epithelium and lamina propria were determined by flow cytometry. Given the diverse cell types that populate the intestine, we were interested in examining potential alterations in the percentage of the different cell populations within the epithelium and LP compartments following AChE inhibition in a non-infected model. After a 3-week treatment with saline, paraoxon or rivastigmine, intestinal tissues were processed, ileal hematopoietic cells (from epithelium and LP) isolated, stained with specific antibodies and analyzed by multicolor flow cytometry. All data analysis was made on single live cells. Supplementary Figs. 5 and 6 depict flow cytometry dot-plots showing the gating strategy used to identify total (SFig. 5A, SFig. 6A) and $CD103^+$ resident (SFig. 5B, SFig. 6B) hematopoietic populations in the intraepithelial and LP compartments.

3.6.1. Intraepithelial compartment

In saline-treated animals, 37.3 % of IE cells consisted of $CD45^+$ hematopoietic cells (Fig. 7A), of which the great majority (72 %) were $CD3^+$ T lymphocytes (Fig. 7B), with only 6.6 % $CD19^+$ B cells (Figs. 7C) and 4.6 % $CD11b^+$ myeloid cells (Fig. 7D). Compared to the saline group, treatment with paraoxon induced a statistically significant increment in the total percentage of hematopoietic cells (49.4 %) in the IE compartment (Fig. 7A) that was not associated with any alteration in the percentage of any of the lymphoid or myeloid subpopulations (Fig. 7B–D). Noticeably, however, rivastigmine treatment resulted in a 30 % decrease in the percentage of hematopoietic cells in IE compartment compared to control group, but without significant alterations in the ratios of the different cell

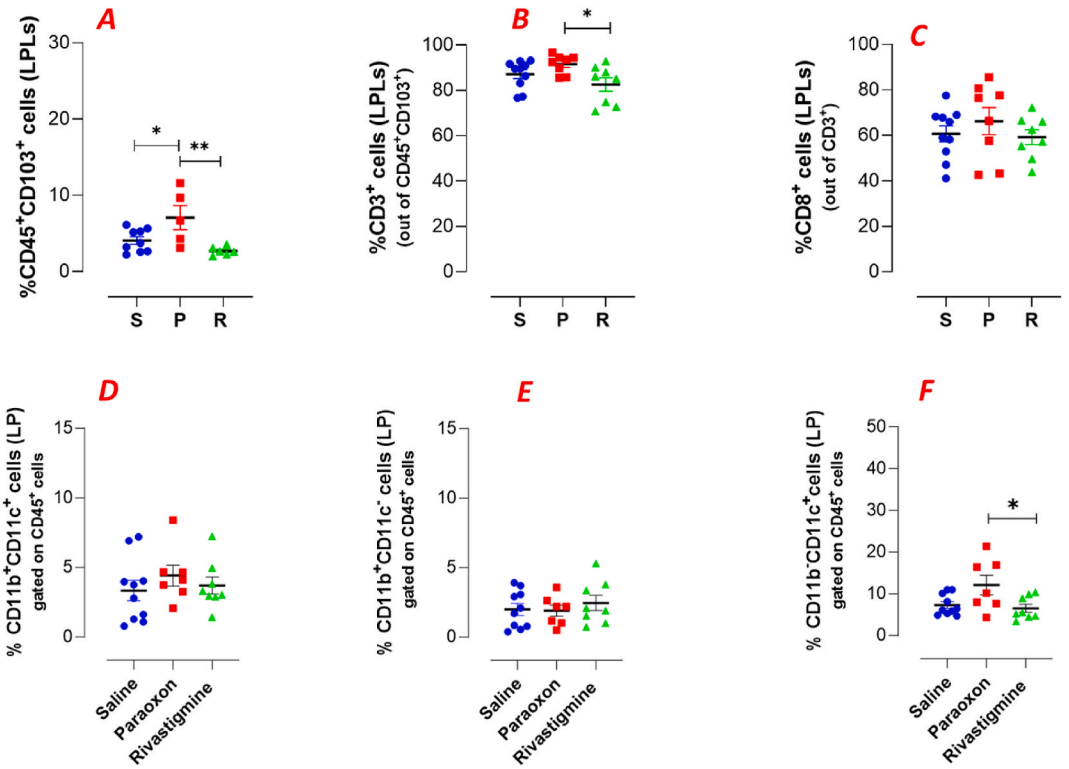

Fig. 8. Phenotypic characterization of resident hemopoietic cells in the intestinal lamina propria. Isolated lamina propria (LP) cells from ileum of control and experimental groups were analyzed by flowcytometry using specific mAbs. (***A-C***) Graphs depict percentages of lamina propria resident (***A***) $CD45^+$ $CD103^+$cells, (***B***) $CD3^+$ T cells and (***C***) $CD8^+$ T cells in each group. In graphs ***D-F*** the percentages of (***D***) $CD11b^+CD11c^+$, (***E***) $CD11b^+CD11c^-$ and (***F***) $CD11b^-CD11c^+$ cells (all populations out of $CD45^+$ cells) in the lamina propria of saline-, paraoxon- and rivastigmine-treated groups. All graphs represent values and mean ± SEM of 5–10 individual mice per group from 3 independent experiments. One-way ANOVA statistical test was used for data analysis. Asterisks denote statistically significant differences between the indicated groups (*$p < 0.05$; **$p < 0.01$).

subpopulations (Fig. 7A–D). Representative dot plots for the three different subpopulations are shown in SFig. 7.

CD103 is an integrin involved in cell-to-cell, and cell-to-matrix interactions [35] and mediates cell adhesion, migration, and lymphocyte homing [36]. Given that CD103 is an important marker for tissue-resident cells in the GI tract, we focused on $CD103^+$ cells in our analysis of possible cellular perturbations induced by the different treatments. Fig. 7E shows a statistically significant increment in the percentage of the total $CD103^+$ population in the paraoxon-treated group (37.8 %) compared to the saline group (27 %) in the IE compartment. On the contrary, following rivastigmine treatment this population decreased by 18.9 % compared to control, but the difference was not statistically significant. In all three groups, however, the majority (92–94 %) of these IE resident cells were identified as T cells (Fig. 7F), probably representing effector/memory T cells that play an important role in host defense against infection [37]. The IE T cell population ($CD45^+CD3^+CD103^+$) was further characterized based on the expression of CD4 and CD8α proteins. We concentrated on the most prominent T cell population within this compartment, namely $CD8^+$ T cells. In saline-treated animals, 70 % of the total resident T cells were $CD8^+$ T cells. Compared to the saline group, paraoxon and rivastigmine treatment induced a small but insignificant increase in the percentage (79 % and 75 %, respectively) of these cells (Fig. 7G). Representative dot plots of these populations are shown in SFig. 8A–C. When expressed as a percentage of the total IEL population, the findings show that paraoxon induced a statistically significant increment in the percentage of $CD8^+CD103^+$ cells (mean ± SEM = 31.7 ± 4.9) compared to control (18.5 ± 1.7), corresponding to an increase of almost 59 % (Fig. 7H). In contrast, the abundance of $CD8^+CD103^+$ cells in rivastigmine-pretreated mice was slightly decreased (11.6 ± 1.8) compared to control (Fig. 7H).

The CD8 coreceptor is a transmembrane dimeric protein that can be expressed as CD8αα homodimer or CD8αβ heterodimer in the intestinal mucosa [38]. Furthermore, the majority of mucosal T cells express the αβ T cell receptor (TCRαβ T cells). A second, minor, population of T cells express γδ TCR (TCRγδ T cells). Thus, based on the differential expression of CD8 and TCR proteins, and the panel of monoclonal antibodies used in our staining protocol, at least three different subpopulations of resident $CD8^+$ T cells could be discerned in the small intestine: $CD8\alpha\alpha^+/TCR\gamma\delta^+$ cells, $CD8\alpha\alpha^+/TCR\alpha\beta^+$ cells, and $CD8\alpha\beta^+/TCR\alpha\beta^+$ T cells (SFig. 9, SFig. 8D). When comparing the percentages of any of these three T cell subpopulations in experimental vs control groups, no statistically significant changes were found (SFig. 9A–C). Considering the increment of resident $CD45^+$ and $CD8^+$ T cells induced by paraoxon treatment, we can conclude that all three $CD8^+$ T subpopulations have undergone a significant increase in abundance following paraoxon, but not rivastigmine, treatment.

3.6.2. Lamina propria compartment

We carried out an extensive phenotypic analysis of cells isolated from the LP compartment using multiple panels of antibodies to lymphoid and myeloid cell populations. In our hand, the isolated cells of the LP compartment in control mice typically consisted of ~27 % $CD45^+$ hematopoietic cells out of which ~25 % were $CD3^+$ T cells, 36 % $CD19^+$ B cells and ~5 % $CD11b^+$ myeloid cells, while 30–35 % of the LP $CD45^+$ cells were not typable using our antibody panels (SFig. 10A–D). Neither paraoxon nor rivastigmine treatment induced major alterations in the percentage of the various $CD45^+$ cell populations. Representative dot plots of these populations are shown in SFig. 11. We then focused on $CD45^+$ $CD103^+$ resident LP cells, which constituted only 4 ± 0.5 % (mean ± SEM) of the total isolated cells or ~15 % of the total $CD45^+$ hematopoietic cells in control mice (Fig. 8A). Paraoxon treatment induced a significant increase (7 ± 1.5 %) in this population (corresponding to ~25 % of the total $CD45^+$ hematopoietic cells) in contrast with rivastigmine treatment where this population decreased significatively to 2.5 ± 0.2 % (~9 % of the total $CD45^+$ hematopoietic cells) (Fig. 8A). The majority of these resident cells were $CD3^+$ T cells in all groups (Fig. 8B). Interestingly, we observed a significant increase in the percentage of resident T cells following paraoxon treatment (average of 92 ± 1.45 %) in comparison to the rivastigmine (82 ± 3 %) group but not to the saline (87 ± 1.9 %) group (Fig. 8B). The majority of these $CD3^+$ cells (60–66 %) were $CD8^+$ T cells in all groups (Fig. 8C). Representative dot plots of these cell populations are shown in SFig. 12 A,B Furthermore, quantitative analysis of the different $CD8^+$ subpopulations, namely $CD8\alpha\alpha^+/TCR\gamma\delta^+$, $CD8\alpha\alpha^+/TCR\gamma\delta^-$ and $CD8\alpha\beta^+$ cells, revealed no significant alterations between saline and neither of the treated experimental groups (SFig.12 C,D and SFig. 13 A-C).

We analyzed the myeloid cell population in the lamina propria based on the differential expression of CD11b and CD11c protein markers. Three distinct subpopulations could be identified (Fig. 8D–F), $CD11b^+CD11c^+$ dendritic cells (DCs), $CD11b^+CD11c^-$ and $CD11b^-CD11c^+$. Our results showed that the $CD11b^+$ populations, $CD11c^+$ and $CD11c^-$, represented ~3 % and 2 %, respectively, of the $CD45^+$ cells in the saline group (Fig. 8D and E). The abundance of these cell populations was not significantly altered by paraoxon nor rivastigmine treatment. On the other hand, $CD11b^-$ $CD11c^+$ population represented ~7 % of the total $CD45^+$ cells in the saline group (Fig. 8F). After paraoxon treatment, the percentage of this population increased to 12 % while rivastigmine treatment did not induce any change (Fig. 8F). Representative dot plots are shown in SFig. 12E.

Thus, only paraoxon but not rivastigmine treatment resulted in a recruitment of resident hematopoietic cells to the intraepithelial compartment as well as to the lamina propria. These resident cells were mostly $CD8^+$ T cells. Additionally, paraoxon treatment led to an increment in $CD11b^-$ $CD11c^+$ population in the lamina propria.

4. Discussion

We have previously demonstrated that exposure to paraoxon, an organophosphorus compound and specific inhibitor of the enzyme AChE, increased survival of mice that were orally infected with a virulent strain of *Salmonella* [26]. In the present study, we investigated whether rivastigmine, an ACh inhibitor used in humans for the treatment of dementia in Alzheimer's and Parkinson's diseases, can also efficiently rescue mice from succumbing to a lethal *Salmonella* infection.

Rivastigmine is a relatively weak (IC_{50} = 4.5 μM) pseudo-irreversible cholinesterase inhibitor that has a safe profile in humans. Rivastigmine binds to the catalytic site of two enzymes, AChE and butyrylcholinesterase (BChE), inhibiting their hydrolytic activity that leads to a delay in the breakdown of ACh in the synaptic cleft. However, the precise mechanism of action is not completely understood yet [39–42]. Rivastigmine has a short half-life (1.5 h) and short pharmacodynamic effect (10 h) [43] and, therefore it is difficult to observe variations in the weekly enzymatic activity of the AChE in red blood cells during the treatment period, as typically observed following paraoxon treatment where the enzymatic activity of AChE is reduced by 50 % after one week of treatment [21,27]. So, instead, the effectiveness of the rivastigmine treatment was validated by following the animal's body weight during the course of the treatment, as it is known that cholinergic stimulation, or increased levels of ACh, induces an increase in animal's physical activity and in the intestinal peristaltic movement that leads to a slower body growth [21,27,32]. Our data showed that rivastigmine reduced the body growth of treated animls, confirming the efficacy of AChE inhibition.

It is noteworthy that in our experimental *Salmonella* model rivastigmine was not able to save treated animals from succumbing to an oral infection with *S. typhimurium* despite the small but significant enhancement in survival. The fact that at day 3 post-infection, systemic organs of rivastigmine-treated mice contained less bacteria than their feces and intestinal content suggests the existence of an effective intestinal barrier that limits the translocation of bacteria to the intestinal mucosa and their subsequent systemic dissemination. However, this effect is only transitory as eventually all infected mice succumbed to the infection. This outcome is in sharp contrast to the good level of protection observed in animals treated with paraoxon where ~80 % of mice survive up to 60 days following infection [27]. However, previous studies have shown that rivastigmine ameliorated clinical symptoms of experimental autoimmune encephalomyelitis (EAE) and reduced the production of pro-inflammatory cytokines in mice [44]. Moreover, in a model of dextran sodium sulphate (DSS)-induced colitis in mice, rivastigmine reduced gastrointestinal inflammation, disease severity and colon damage [45]. The same DSS mouse model was used by another group to demonstrate that pyridostigmine, another AChE inhibitor, reduced eosinophilic infiltration, increased mucin production and improved epithelial integrity [46].

When oral pathogens try to invade the intestinal mucosa, the first obstacle they encounter is the mucus layer covering the gastrointestinal epithelium where the microbes are halted, trapped and then removed by peristalsis [47]. The goblet cells are essential members of the intestinal innate defense mechanism that maintain intestinal homeostasis [48], and are responsible for the synthesis and secretion of mucins, the main component of the mucus layer [49]. The binding of ACh to the M3 muscarinic receptors expressed on goblet cells induces the mobilization of Ca^{2+} in the cytoplasm [50], resulting in mucus secretion [51] by compound exocytosis that induces the fusion and secretion of multiple pre-formed apically stored mucin-containing granules [51,52]. Herein we demonstrate that, similar to what was previously observed with paraoxon [27], treatment with rivastigmine induced goblet cell degranulation and

the release of mucin, which explains the increased thickness of the intestinal mucus layer. The mucus layer also contains a variety of host defense peptides, secreted by the Paneth cells located at the base of the small intestinal crypts [53]. In response to microbial antigens, Paneth cells release the content of their secretory granules, rich in anti-microbial peptides and proteolytic enzymes like lysozyme, to the intestinal lumen [54,55]. Moreover, Paneth cells express muscarinic AChRs [56] and are able to degranulate following stimulation with carbamylcholine, an acetylcholine receptor agonist [57]. Similarly, herein we report that treatment with either paraoxon or rivastigmine induced the degranulation of Paneth cells and release of lysozyme to the intestinal lumen [27]. However, we cannot discard the possibility of a direct interaction between rivastigmine or paraoxon with the Paneth and goblet cells that could induce their degranulation for which further *in vitro* studies are needed. Taken together, our results indicate that rivastigmine acts in an analogous manner to paraoxon insofar as its ability to induce an effective intestinal barrier that could delay the translocation of pathogens to the intestinal mucosa, hence providing a rationale for the increased survival of *Salmonella*-infected animals. However, unlike paraoxon which provided long term protection against virulent *Salmonella* in 80 % of mice [26,27], rivastigmine-treated mice could not be fully protected against the lethal infection. This suggests that paraoxon and rivastigmine could act differentially on other compartments of the gut-associated lymphoid tissue.

IELs and LPLs form very specialized lymphoid compartments that regulate the intestinal immune response to infection (reviewed in Ref. [58]). These compartments are phenotypically and functionally distinct due to their diverse cell populations (Reviewed in Ref. [59]. IELs consist mainly of resident $CD103^+CD8^+$ T cells [60–62], located among the basolateral surface of the epithelial cells, at the intersection between the external and internal environment [63,64] which allows them to monitor the intestinal microbiota. Functionally, these cells maintain mucosal homeostasis by continuous surveillance of the intestine and act as immunoregulatory effectors with potent cytolytic activity protecting host tissues from infection and uncontrolled systemic infiltration [65,66]. Our findings show that paraoxon treatment led to a significant increase in the percentage of $CD103^+CD8^+$ cells in the ileal mucosa, providing a reinforcement of this first line of cellular immune defense [67]. In this regard, $CD8^+$ T cells have been shown to prevent early systemic dissemination of *Y. enterocolitica* [68] and play an essential role in *Salmonella* clearance [69]. Studies on patients with inflammatory bowel disease (IBD) reported low percentages of $CD103^+$ T cells in comparation to healthy controls [70] and a shift toward more $CD103^-$ T cells during active inflammation [71]. Therefore, expansion in the percentage of $CD103^+CD8^+$ cells in the intestinal mucosa represents a clear advantage for a rapid and efficient host response to an infection. Contrary to paraoxon, rivastigmine treatment did not induce any increase in these populations which could indicate that more persistent high levels of ACh are needed to induce changes on the mucosal immune cell populations.

CD11c is an integrin molecule expressed typically on dendritic cells and, therefore, is considered a typical marker for dendritic cells [72]. However, CD11c can also be expressed on other cell populations like activated T and B lymphocytes as well as NK cells [73]. Several studies had tried to elucidate the role of CD11c on these cells and although it seems to be correlated with higher cytotoxicity and effector or regulatory functions [74], it is still unclear. The fact that paraoxon treatment resulted in an increase in the percentage of $CD11c^+CD11b^-$ cells in the intestinal LP could indicate that these cells are not the typical dendritic cells, instead they are probably $CD8^+$ cells (unpublished data) as it was reported by others [75]. Moreover, some studies correlated the expression of CD11c with a T cell population that gets expanded in response to infection [76]. An increase of CD11c expression on T cells of uninfected mice would indicate an activation and/or migration of these cells to the LP and constitute an advantage to the host for a more rapid adaptive immune response to a potential infection, when the effector responses are essential. Further studies are needed to investigate the direct effect of ACh on the expression of CD11c integrin. Similar to $CD8^+CD103^+$ cells, the increase of $CD11b^-CD11c^+$ cells was not observed in the intestinal mucosa of rivastigmine-treated mice, suggesting that high levels of ACh in the intestinal microenvironment promote the expression of CD103 and, probably, CD11c on T cells in the intestinal mucosa.

These results suggest that $CD8^+$ T and $CD11b^-CD11c^+$ cells are able to respond to the elevated levels of ACh induced by the inhibition of AChE. T and B lymphocytes as well as DCs and macrophages, express muscarinic and nicotinic receptors [11] and other components (ChAT, AChE) necessary for a functional, non-neuronal cholinergic system [12,13]. Thus, ACh could play a role in regulating immune cell functions, thereby modulating the immune response. In fact, multiple studies have shown that, upon activation, T and B cells can produce ACh which may contribute to immune responses in several possible ways, by modulating macrophage function [12], controlling neutrophil recruitment [13], regulating intestinal AMP secretion [77], inducing T cell migration [78] and increasing vasodilation [79]. Inhibition of AChE activity could modulate mucosal immune system cells through (a) a direct interaction of their AChR with ACh or (b) indirect thorough products (cytokines, chemokines, etc) secreted by other cells in response to ACh. Another possibility to consider is that the increase in mucin and AMP secretion induced by AChE inhibition could influence the microbiota composition which in turn could modulate the cellular composition of the intestinal mucosa. However, much needs to be done to clearly understand how AChE inhibition regulates the complex immune cellular network existing in the intestinal mucosa.

Independently of the source of ACh (neuronal or non-neuronal), our data suggest that elevated levels of ACh induced an increase in the percentage of $CD8^+$ tissue resident T cells ($CD8^+CD103^+$). These cells are retained in the mucosa in a semi-activated state or "poised activation state" as they not only express genes associated with cytotoxic T cells (Granzyme A and B, Reg3γ) but also express transcripts of genes involved in immune regulation such as CTLA4 and Ly49E-G [80,81]; importantly, however, they lack expression of cytokines [81]. The activation status of IELs is thought to be maintained by factors in the local environment. In fact, lymphocytes in the intestinal mucosa, specially IELs, express receptors for TGFβ, IL-15 and IL-7, all secreted by IECs. TGFβ is involved in the maintenance of IELs and induction of CD103 expression [82], while IL-15 triggers IELs to became cytotoxic [83,84] and IL-7 regulates their survival and proliferation [85]. Considering that IECs express different subtypes of muscarinic ACh receptors [86], we could hypothesize that persistent high levels of ACh not only stimulate the production of mucins and lysozyme from goblet and Paneth cells, respectively, but also could induce IECs to produce cytokines such TGFβ, IL-15 and IL-7 that would induce the expression of CD103 and CD11c on $CD8^+$ T cells, thereby promoting their proliferation in the intestinal mucosa (Fig. 9). Given that the expression of CD11c on T cells is also

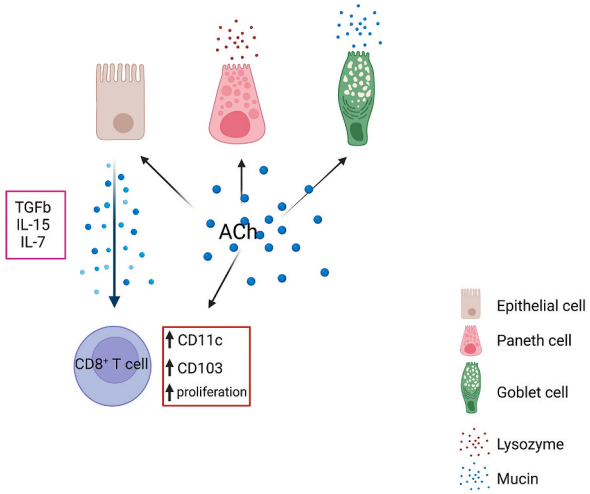

Fig. 9. Graphic representation of possible mechanism by which ACh modulates the resident CD8 population in the intestinal mucosa. Created with BioRender.

associated with mucosal homing and activated state [87], the expression of both CD103 and CD11c would enable $CD8^+$ T cells to quickly respond to an infection, modulating the initial response and recruitment of other immune cells. Although, to the best of our knowledge, there are no reports describing a direct effect of ACh on the expression of CD103 or CD11c on T cells, we cannot rule out the possibility that these proteins may also be modulated through the direct action of ACh on these cells.

Our results demonstrate that although paraoxon and rivastigmine both inhibit the activity of the AChE, they act differentially on the intestinal mucosa. This can be due to several factors: (a) paraoxon is an irreversible AChE inhibitor while rivastigmine is a reversible AChE inhibitor. This means that paraoxon-treated mice would be exposed to a more prolonged inhibition of AChE activity and, therefore, higher levels of ACh than mice treated with rivastigmine; (b) the plasma half-life of paraoxon is 20 h [88] while for rivastigmine is only 1.5 h [43] which means that the elevated levels of ACh (induced by AChE inhibition) are more constant following paraoxon administration than rivastigmine; (c) rivastigmine can cross the blood-brain barrier (BBB) but not paraoxon for which paraoxon would exert its effect only in the periphery. In fact, it has been described that rivastigmine is quite specific and acts mostly on the AChE in the brain compared to the peripheral tissues [89] which could indicate that in our model, the effect observed in the GI tract of paraoxon-treated mice does not involve directly the central nervous system (CNS). Finally, we would like to comment on the observation that high percentage of the $CD45^+$ cells in the LP lack antigen-specific receptor ($CD3^-CD19^-CD11b^-$), as previously reported by others [90], suggesting the presence of other cells including innate lymphoid cells (ILCs), important for immuno-surveillance and cytokine response [91,92]. We are currently investigating this possibility.

In the current study, we attempted to shed light on the potential reasons for the differential outcome on protection afforded by paraoxon and rivastigmine by assessing the alterations in the mucosal immune system induced by either treatment in non-infected mice. We reasoned that carrying out this analysis in mice treated only with the different inhibitors may provide clues as to why paraoxon-treated mice survive a lethal infection while rivastigmine treatment fails to do so. We hypothesized that cholinergic stimulation by AChE inhibitors may create a mucosal environment less favorable for the growth of *Salmonella* and more able to resist bacterial infection. We are cognizant of the fact that any observed changes in mucosal immune system in non-infected mice may not be the same as in infected animals. To address this, we would need to carry out a thorough analysis in the context of drug treatment and infection. Based on the present findings, we propose that a sustained and, perhaps, more peripheral cholinergic stimulation by AChE inhibitors could modulate the immune cell populations in charge of surveillance and recognition of invading pathogens, allowing them to mount a quick and efficient response. Overall, our data suggest that peripheral AChE inhibitors (such as paraoxon) create a robust anti-pathogen environment in the intestinal mucosa, not only in the epithelium but more importantly in the LP where the invading pathogens need to be stopped to avoid systemic dissemination, rendering the host more resistant to pathogen invasion. However, given the complexity of mucosal cell interactions that could take place following AChE inhibition, more exhaustive investigations are needed. Our results indicate the possibility of a new cellular mechanism in which AChE inhibition leads to increased accumulation of $CD8^+$ T cells within the intestinal mucosa, thus highlighting a new modality for mobilizing T cells in the GI tract. This assumption would support cholinergic stimulation as a useful therapeutic approach to modulate the immune mechanisms underlying inflammatory processes.

Data availability

The data supporting the findings of this study are available within the article and its supplementary material. Further inquiries can be directed to the corresponding author.

Ethics statement

The animal studies were reviewed and approved by the institutional Animal Research Ethics Committee of United Arab Emirates University.

CRediT authorship contribution statement

Alreem Al-Mansori: Writing – original draft, Visualization, Validation, Investigation. **Ashraf Al-Sbiei:** Visualization, Investigation, Formal analysis. **Ghada H. Bashir:** Visualization, Investigation. **Mohammed M. Qureshi:** Investigation. **Saeed Tariq:** Investigation. **Abeer Altahrawi:** Formal analysis. **Basel K. al-Ramadi:** Writing – review & editing, Visualization, Formal analysis. **Maria J. Fernandez-Cabezudo:** Writing – review & editing, Visualization, Supervision, Resources, Funding acquisition, Formal analysis, Conceptualization.

Declaration of competing interest

The authors declare that they have no known competing financial interests or personal relationships that could have appeared to influence the work reported in this paper.

Acknowledgments

The authors wish to acknowledge the United Arab Emirates Univerity (UAEU) for supporting this project through grant #31M309 from the UAEU Program for Advanced Research, and grant #31M427 from the Research Grants Committee of the College of Medicine and Health Sciences, UAEU,awarded to M.J.F-C. This work formed part of the thesis dissertation for the award of the MSc degree to A. A-M.

Appendix A. Supplementary data

Supplementary data to this article can be found online at https://doi.org/10.1016/j.heliyon.2024.e33849.

References

[1] H.F. Helander, L. Fandriks, Surface area of the digestive tract - revisited, Scand. J. Gastroenterol. 49 (6) (2014) 681–689.
[2] P. Brandtzaeg, R. Pabst, Let's go mucosal: communication on slippery ground, Trends Immunol. 25 (11) (2004) 570–577.
[3] M. Cobo-Simon, R. Hart, H. Ochman, Gene flow and species boundaries of the genus Salmonella, mSystems 8 (4) (2023) e0029223.
[4] A.K. Singh, et al., Streptomycin induced stress response in Salmonella enterica serovar typhimurium shows distinct colony scatter signature, PLoS One 10 (8) (2015) e0135035.
[5] A.D. Teklemariam, et al., Human salmonellosis: a continuous global threat in the farm-to-fork food safety continuum, Foods 12 (9) (2023).
[6] R.J. Phillips, T.L. Powley, Innervation of the gastrointestinal tract: patterns of aging, Auton. Neurosci. 136 (1–2) (2007) 1–19.
[7] H.R. Berthoud, et al., Vagal sensors in the rat duodenal mucosa: distribution and structure as revealed by in vivo DiI-tracing, Anat. Embryol. 191 (3) (1995) 203–212.
[8] T.L. Powley, et al., Gastrointestinal tract innervation of the mouse: afferent regeneration and meal patterning after vagotomy, Am. J. Physiol. Regul. Integr. Comp. Physiol. 289 (2) (2005) R563–R574.
[9] K.Z. Sato, et al., Diversity of mRNA expression for muscarinic acetylcholine receptor subtypes and neuronal nicotinic acetylcholine receptor subunits in human mononuclear leukocytes and leukemic cell lines, Neurosci. Lett. 266 (1) (1999) 17–20.
[10] R.W. Saeed, et al., Cholinergic stimulation blocks endothelial cell activation and leukocyte recruitment during inflammation, J. Exp. Med. 201 (7) (2005) 1113–1123.
[11] K. Kawashima, et al., Expression and function of genes encoding cholinergic components in murine immune cells, Life Sci. 80 (24–25) (2007) 2314–2319.
[12] M. Rosas-Ballina, et al., Acetylcholine-synthesizing T cells relay neural signals in a vagus nerve circuit, Science 334 (6052) (2011) 98–101.
[13] C. Reardon, et al., Lymphocyte-derived ACh regulates local innate but not adaptive immunity, Proc. Natl. Acad. Sci. U. S. A. 110 (4) (2013) 1410–1415.
[14] L.V. Borovikova, et al., Vagus nerve stimulation attenuates the systemic inflammatory response to endotoxin, Nature 405 (6785) (2000) 458–462.
[15] K.J. Tracey, The inflammatory reflex, Nature 420 (6917) (2002) 853–859.
[16] M. Rosas-Ballina, et al., The selective alpha7 agonist GTS-21 attenuates cytokine production in human whole blood and human monocytes activated by ligands for TLR2, TLR3, TLR4, TLR9, and RAGE, Mol. Med. 15 (7–8) (2009) 195–202.
[17] V.A. Pavlov, S.S. Chavan, K.J. Tracey, Molecular and functional neuroscience in immunity, Annu. Rev. Immunol. 36 (2018) 783–812.
[18] J. Meregnani, et al., Anti-inflammatory effect of vagus nerve stimulation in a rat model of inflammatory bowel disease, Auton. Neurosci. 160 (1–2) (2011) 82–89.
[19] Y.A. Levine, et al., Neurostimulation of the cholinergic anti-inflammatory pathway ameliorates disease in rat collagen-induced arthritis, PLoS One 9 (8) (2014) e104530.
[20] J.M. Huston, et al., Transcutaneous vagus nerve stimulation reduces serum high mobility group box 1 levels and improves survival in murine sepsis, Crit. Care Med. 35 (12) (2007) 2762–2768.
[21] J.A. George, et al., Cholinergic stimulation prevents the development of autoimmune diabetes: evidence for the modulation of Th17 effector cells via an IFNgamma-dependent mechanism, Front. Immunol. 7 (2016) 419.
[22] V.A. Pavlov, et al., Brain acetylcholinesterase activity controls systemic cytokine levels through the cholinergic anti-inflammatory pathway, Brain Behav. Immun. 23 (1) (2009) 41–45.
[23] G.S. Pham, K.W. Mathis, Lipopolysaccharide challenge reveals hypothalamic-pituitary-adrenal Axis dysfunction in murine systemic lupus erythematosus, Brain Sci. 8 (10) (2018).
[24] P.S. Olofsson, et al., Blood pressure regulation by CD4(+) lymphocytes expressing choline acetyltransferase, Nat. Biotechnol. 34 (10) (2016) 1066–1071.

[25] H. Wang, et al., Nicotinic acetylcholine receptor alpha7 subunit is an essential regulator of inflammation, Nature 421 (6921) (2003) 384–388.
[26] M.J. Fernandez-Cabezudo, et al., Cholinergic stimulation of the immune system protects against lethal infection by Salmonella enterica serovar Typhimurium, Immunology 130 (3) (2010) 388–398.
[27] R.M. Al-Barazie, et al., Cholinergic activation enhances resistance to oral Salmonella infection by modulating innate immune defense mechanisms at the intestinal barrier, Front. Immunol. 9 (2018) 551.
[28] M.J. Fernandez-Cabezudo, et al., Involvement of acetylcholine receptors in cholinergic pathway-mediated protection against autoimmune diabetes, Front. Immunol. 10 (2019) 1038.
[29] M.B. Colovic, et al., Acetylcholinesterase inhibitors: pharmacology and toxicology, Curr. Neuropharmacol. 11 (3) (2013) 315–335.
[30] B.K. al-Ramadi, et al., Cytokine expression by attenuated intracellular bacteria regulates the immune response to infection: the Salmonella model, Mol. Immunol. 38 (12–13) (2002) 931–940.
[31] B.K. al-Ramadi, et al., Activation of innate immune responses by IL-2-expressing Salmonella typhimurium is independent of Toll-like receptor 4, Mol. Immunol. 40 (10) (2004) 671–679.
[32] S.K. Satapathy, et al., Galantamine alleviates inflammation and other obesity-associated complications in high-fat diet-fed mice, Mol. Med. 17 (7–8) (2011) 599–606.
[33] N. Barker, M. van de Wetering, H. Clevers, The intestinal stem cell, Genes Dev. 22 (14) (2008) 1856–1864.
[34] J.P. Ingram, I.E. Brodsky, S. Balachandran, Interferon-gamma in Salmonella pathogenesis: new tricks for an old dog, Cytokine 98 (2017) 27–32.
[35] M.L. del Rio, et al., Development and functional specialization of CD103+ dendritic cells, Immunol. Rev. 234 (1) (2010) 268–281.
[36] G. Fousteri, et al., CD103 is dispensable for anti-viral immunity and autoimmunity in a mouse model of virally-induced autoimmune diabetes, J. Autoimmun. 32 (1) (2009) 70–77.
[37] L. Lefrancois, L. Puddington, Intestinal and pulmonary mucosal T cells: local heroes fight to maintain the status quo, Annu. Rev. Immunol. 24 (2006) 681–704.
[38] H.C. Chang, et al., Structural and mutational analyses of a CD8alphabeta heterodimer and comparison with the CD8alphaalpha homodimer, Immunity 23 (6) (2005) 661–671.
[39] F. Fan, et al., The efficacy and safety of alzheimer's disease therapies: an updated umbrella review, J Alzheimers Dis 85 (3) (2022) 1195–1204.
[40] G. Marucci, et al., Efficacy of acetylcholinesterase inhibitors in Alzheimer's disease, Neuropharmacology 190 (2021) 108352.
[41] I. Vecchio, et al., The state of the art on acetylcholinesterase inhibitors in the treatment of alzheimer's disease, J. Cent. Nerv. Syst. Dis. 13 (2021) 11795735211029113.
[42] T. Jamshidnejad-Tosaramandani, et al., The potential effect of insulin on AChE and its interactions with rivastigmine in vitro, Pharmaceuticals 14 (11) (2021).
[43] J.S. Birks, L.Y. Chong, J. Grimley Evans, Rivastigmine for Alzheimer's disease, Cochrane Database Syst. Rev. 9 (9) (2015) CD001191.
[44] E. Nizri, et al., Suppression of neuroinflammation and immunomodulation by the acetylcholinesterase inhibitor rivastigmine, J. Neuroimmunol. 203 (1) (2008) 12–22.
[45] H. Shifrin, et al., Rivastigmine alleviates experimentally induced colitis in mice and rats by acting at central and peripheral sites to modulate immune responses, PLoS One 8 (2) (2013) e57668.
[46] S.P. Singh, et al., Acetylcholinesterase inhibitor pyridostigmine bromide attenuates gut pathology and bacterial dysbiosis in a murine model of ulcerative colitis, Dig. Dis. Sci. 65 (1) (2020) 141–149.
[47] D.A. Elphick, Y.R. Mahida, Paneth cells: their role in innate immunity and inflammatory disease, Gut 54 (12) (2005) 1802–1809.
[48] H.A. McCauley, G. Guasch, Three cheers for the goblet cell: maintaining homeostasis in mucosal epithelia, Trends Mol. Med. 21 (8) (2015) 492–503.
[49] R. Bansil, B.S. Turner, The biology of mucus: composition, synthesis and organization, Adv. Drug Deliv. Rev. 124 (2018) 3–15.
[50] D. Ambort, et al., Calcium and pH-dependent packing and release of the gel-forming MUC2 mucin, Proc. Natl. Acad. Sci. U. S. A. 109 (15) (2012) 5645–5650.
[51] R.D. Specian, M.R. Neutra, Mechanism of rapid mucus secretion in goblet cells stimulated by acetylcholine, J. Cell Biol. 85 (3) (1980) 626–640.
[52] G.M. Birchenough, et al., New developments in goblet cell mucus secretion and function, Mucosal Immunol. 8 (4) (2015) 712–719.
[53] H.C. Clevers, C.L. Bevins, Paneth cells: maestros of the small intestinal crypts, Annu. Rev. Physiol. 75 (2013) 289–311.
[54] Y. Satoh, L. Vollrath, Quantitative electron microscopic observations on Paneth cells of germfree and ex-germfree Wistar rats, Anat. Embryol. 173 (3) (1986) 317–322.
[55] H. Tanabe, et al., Mouse paneth cell secretory responses to cell surface glycolipids of virulent and attenuated pathogenic bacteria, Infect. Immun. 73 (4) (2005) 2312–2320.
[56] E.D. Muise, et al., Distribution of muscarinic acetylcholine receptor subtypes in the murine small intestine, Life Sci. 169 (2017) 6–10.
[57] Y. Yokoi, et al., Paneth cell granule dynamics on secretory responses to bacterial stimuli in enteroids, Sci. Rep. 9 (1) (2019) 2710.
[58] H. Cheroutre, F. Lambolez, D. Mucida, The light and dark sides of intestinal intraepithelial lymphocytes, Nat. Rev. Immunol. 11 (7) (2011) 445–456.
[59] A.M. Mowat, W.W. Agace, Regional specialization within the intestinal immune system, Nat. Rev. Immunol. 14 (10) (2014) 667–685.
[60] D. Guy-Grand, et al., Two gut intraepithelial CD8+ lymphocyte populations with different T cell receptors: a role for the gut epithelium in T cell differentiation, J. Exp. Med. 173 (2) (1991) 471–481.
[61] L. Lefrancois, Intraepithelial lymphocytes of the intestinal mucosa: curiouser and curiouser, Semin. Immunol. 3 (2) (1991) 99–108.
[62] H. Cheroutre, Starting at the beginning: new perspectives on the biology of mucosal T cells, Annu. Rev. Immunol. 22 (2004) 217–246.
[63] K.A. Brogden, Antimicrobial peptides: pore formers or metabolic inhibitors in bacteria? Nat. Rev. Microbiol. 3 (3) (2005) 238–250.
[64] C.L. Wilson, et al., Regulation of intestinal alpha-defensin activation by the metalloproteinase matrilysin in innate host defense, Science 286 (5437) (1999) 113–117.
[65] A. Hayday, et al., Intraepithelial lymphocytes: exploring the Third Way in immunology, Nat. Immunol. 2 (11) (2001) 997–1003.
[66] D.P. Hoytema van Konijnenburg, et al., Intestinal epithelial and intraepithelial T cell crosstalk mediates a dynamic response to infection, Cell 171 (4) (2017) 783–794 e13.
[67] B. Jabri, V. Abadie, IL-15 functions as a danger signal to regulate tissue-resident T cells and tissue destruction, Nat. Rev. Immunol. 15 (12) (2015) 771–783.
[68] D.T. Siefker, B. Adkins, Rapid CD8(+) function is critical for protection of neonatal mice from an extracellular bacterial enteropathogen, Front Pediatr 4 (2016) 141.
[69] J. Hess, et al., Salmonella typhimurium aroA- infection in gene-targeted immunodeficient mice: major role of CD4+ TCR-alpha beta cells and IFN-gamma in bacterial clearance independent of intracellular location, J. Immunol. 156 (9) (1996) 3321–3326.
[70] C. Smids, et al., Intestinal T cell profiling in inflammatory bowel disease: linking T cell subsets to disease activity and disease course, J Crohns Colitis 12 (4) (2018) 465–475.
[71] B. Roosenboom, et al., Intestinal CD103+CD4+ and CD103+CD8+ T-cell subsets in the gut of inflammatory bowel disease patients at diagnosis and during follow-up, Inflamm. Bowel Dis. 25 (9) (2019) 1497–1509.
[72] D. Ganguly, et al., The role of dendritic cells in autoimmunity, Nat. Rev. Immunol. 13 (8) (2013) 566–577.
[73] A. Arakelyan, et al., Histocultures (tissue explants) in human retrovirology, Methods Mol. Biol. 1087 (2014) 233–248.
[74] S. Tsai, X. Clemente-Casares, P. Santamaria, CD8(+) Tregs in autoimmunity: learning "self"-control from experience, Cell. Mol. Life Sci. 68 (23) (2011) 3781–3795.
[75] M. Kuka, I. Munitic, J.D. Ashwell, Identification and characterization of polyclonal alphabeta-T cells with dendritic cell properties, Nat. Commun. 3 (2012) 1223.
[76] L.A. Cooney, et al., Short-lived effector CD8 T cells induced by genetically attenuated malaria parasite vaccination express CD11c, Infect. Immun. 81 (11) (2013) 4171–4181.
[77] S. Dhawan, et al., Acetylcholine-producing T cells in the intestine regulate antimicrobial peptide expression and microbial diversity, Am. J. Physiol. Gastrointest. Liver Physiol. 311 (5) (2016) G920–G933.
[78] M.A. Cox, et al., Choline acetyltransferase-expressing T cells are required to control chronic viral infection, Science 363 (6427) (2019) 639–644.

[79] L. Tarnawski, et al., Cholinergic regulation of vascular endothelial function by human ChAT(+) T cells, Proc. Natl. Acad. Sci. U. S. A. 120 (14) (2023) e2212476120.
[80] A.M. Fahrer, et al., Attributes of gammadelta intraepithelial lymphocytes as suggested by their transcriptional profile, Proc. Natl. Acad. Sci. U. S. A. 98 (18) (2001) 10261–10266.
[81] J. Shires, E. Theodoridis, A.C. Hayday, Biological insights into TCRgammadelta+ and TCRalphabeta+ intraepithelial lymphocytes provided by serial analysis of gene expression (SAGE), Immunity 15 (3) (2001) 419–434.
[82] J.E. Konkel, et al., Control of the development of CD8alphaalpha+ intestinal intraepithelial lymphocytes by TGF-beta, Nat. Immunol. 12 (4) (2011) 312–319.
[83] B. Meresse, et al., Coordinated induction by IL15 of a TCR-independent NKG2D signaling pathway converts CTL into lymphokine-activated killer cells in celiac disease, Immunity 21 (3) (2004) 357–366.
[84] M. Itsumi, Y. Yoshikai, H. Yamada, IL-15 is critical for the maintenance and innate functions of self-specific CD8(+) T cells, Eur. J. Immunol. 39 (7) (2009) 1784–1793.
[85] H. Yang, A.U. Spencer, D.H. Teitelbaum, Interleukin-7 administration alters intestinal intraepithelial lymphocyte phenotype and function in vivo, Cytokine 31 (6) (2005) 419–428.
[86] C.L. Hirota, D.M. McKay, Cholinergic regulation of epithelial ion transport in the mammalian intestine, Br. J. Pharmacol. 149 (5) (2006) 463–479.
[87] J. Qualai, et al., Expression of CD11c is associated with unconventional activated T cell subsets with high migratory potential, PLoS One 11 (4) (2016) e0154253.
[88] L. Musilova, et al., In vitro oxime-assisted reactivation of paraoxon-inhibited human acetylcholinesterase and butyrylcholinesterase, Clin. Toxicol. 47 (6) (2009) 545–550.
[89] G.T. Grossberg, Cholinesterase inhibitors for the treatment of Alzheimer's disease:: getting on and staying on, Curr. Ther. Res. Clin. Exp. 64 (4) (2003) 216–235.
[90] A. Valle-Noguera, et al., Optimized protocol for characterization of mouse gut innate lymphoid cells, Front. Immunol. 11 (2020) 563414.
[91] J. Mjosberg, H. Spits, Human innate lymphoid cells, J. Allergy Clin. Immunol. 138 (5) (2016) 1265–1276.
[92] M. Ebbo, et al., Innate lymphoid cells: major players in inflammatory diseases, Nat. Rev. Immunol. 17 (11) (2017) 665–678. DIAGRAMS.